Measured Index of Refraction for Argon Plasma*

W. F. Hug, D. Evans, R. S. Tankin, and A. B. Cambel†
Gas Dynamics Laboratory, Northwestern University, Evanston, Illinois
(Received 22 July 1966; revised mansucript received 17 April 1967)

The index of refraction of argon plasma in the temperature range 9500 to 19 000°K was measured at a wavelength of 6328 Å. A helium-neon laser was used as the light source for a Mach-Zehnder interferometer. A modified commercial plasma jet and a free-burning arc were used as plasma sources. The index of refraction was calculated using the Slater screening-constant method. The measured index of refraction lies between the theoretical curve which considers contributions from only ground-state atoms and free electrons and the curve which considers excited electrons as free. There appears to be a lowering of the ionization limit to a principle quantum number of 5 for the atom of 16 000°K, compared with Olsen's value of 6.

I. INTRODUCTION

THE interferometer is used to measure phase index of refraction, which in turn can be related to the thermophysical state of the gas. For neutral gases, the relation between the phase index of refraction and density is well known and the interferometer has proved useful in studying gases having temperatures up to about 5000°K. In this temperature regime, the phase index of refraction (or measured phase displacement) is a strong function of gas density. Consequently, precise density measurements can be made. At temperatures in excess of 5000°K, when only ground-state atoms and free electrons (neglecting excited-state contributions) are considered, the calculated index of refraction is weakly temperature-dependent. Therefore, small errors in phase-shift measurements will result in large errors in number densities. However, the assumption that the refractive index is determined by ground-state atoms and free electrons yields a dispersion relation that is predominately due to free electrons. With this assumption, two interferograms obtained at two different wavelengths would yield the electron concentration in the plasma. It follows that for an equilibrium plasma the entire physical state of the plasma can be defined, if the dispersion in the refractive index is caused by the free electrons alone. Such an assumption has been used by Alpher and White[1] to interpret their experimental results. Since an arc-heated plasma is composed of ground-state atoms, ions, free electrons, excited atoms, and excited ions, it is desirable to examine the contributions of the excited states to the index of refraction both analytically and experimentally.

II. THEORETICAL CONSIDERATIONS

The index of refraction μ is a directly measurable property of the plasma which is related to the phase velocity of light by

$$\mu = c/v, \tag{1}$$

where c is the phase velocity of light in a vacuum and v is the phase velocity of light in the plasma. The contribution to the index of refraction of the bound and free electrons will be studied separately. There is little difficulty in determining the free-electron contribution, but the bound-electron contribution is another matter. Two different approaches to calculate the contribution to the index of refraction due to the bound electron are examined. In these calculations it is assumed that the plasma is in equilibrium and that the component configurations do not interact with each other.[2] For this condition the index of refraction may be written as

$$\mu - 1 = 2\pi \sum_i \alpha_i N_i, \tag{2}$$

where α_i is the polarizability of the ith configuration, N_i is the number density of the ith configuration, and the summation is over all configurations present in the plasma. The term "configuration" refers to the particular distribution of bound electrons of a species. The polarizability of a configuration is defined as the induced dipole moment of that configuration per unit electric-field strength applied to the plasma. The dipole moment is the product of an electronic charge and its separation from an equilibrium position.

The polarizability of a bound set of electrons has been formulated classically by Drude[3] and quantum mechanically by Ladenburg.[4] The formulations are equivalent, the Drude formulation being

$$\alpha(v) = \frac{e^2}{4\pi^2 m} \sum_i \frac{f_i}{\nu_i^2 - \nu^2}, \tag{3}$$

where e and m are, respectively, the charge and mass of an electron, f_i is the oscillator strength of the ith transition, ν_i is the characteristic frequency of the ith transition, and ν is the illumination frequency.

There are two limiting cases: first, where the illumination frequency is very high compared to the ν_i; and second, where the illumination frequency is very low compared to the ν_i. In the first case, the bound electrons appear as free and have the polarizability of free

* Research supported by the Aeronautical Research Laboratories, Wright-Patterson U. S. Air Force Base.
† On leave as Director, Research and Engineering Support Division, Institute for Defense Analysis, Arlington, Virginia.
[1] R. A. Alpher and D. R. White, Phys. Fluids **2**, 162 (1959).
[2] R. H. Huddelstone and S. L. Leonard, *Plasma Diagnostic Techniques* (Academic Press Inc., New York, 1965).
[3] J. O. Hirshfelder, C. F. Curtiss, and R. B. Bird, *Molecular Theory of Gases and Liquids* (John Wiley & Sons, Inc., New York, 1965).

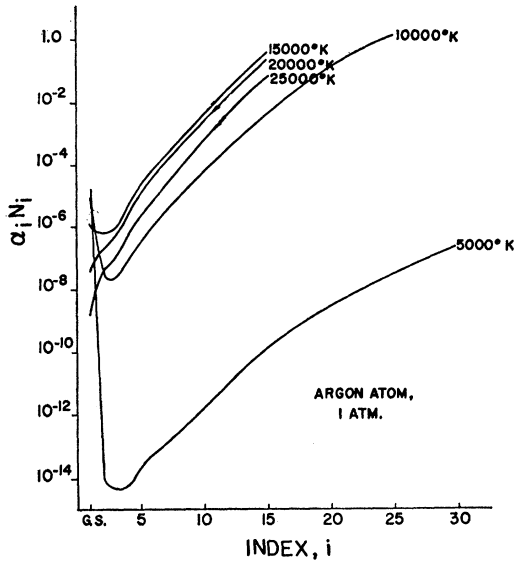

FIG. 1. Excited-state contributions to index of refraction.

electrons.

$$\alpha(\nu) = -e^2/4\pi^2 m\nu^2, \tag{4}$$

where $\nu \gg \nu_i$. On the other hand, at very low illumination frequencies, the polarizability of the bound set of electrons is limited by the ionization limit. In this case[3]

$$\alpha(0) = \frac{4}{9a_0} \sum_{i=1}^{t} \langle r_i^2 \rangle_{\mathrm{av}}^2, \tag{5}$$

where r_i is the ith electron orbit radius, a_0 is the first Bohr radius, and t is the ionization limit. The mean-square radius is

$$\langle r_i^2 \rangle_{\mathrm{av}} = [n^*{}_i/2Z^*](2n_i^*+1)(2n_i^*+2)a_0^2, \tag{6}$$

where $n^*{}_i$ is the effective principal quantum number and Z^* is the effective nuclear charge. This is reviewed in Ref. 3.

The measured polarizability of the ground-state argon atom is reported to be $11.04a_0^3$ by Knox[5] and $11.28a_0^3$ by Raleigh.[6] The value used in this study is $11.25a_0$.[3] Equations (5) and (6) are used to calculate the excited-state polarizabilities. The polarizabilities of the atomic and first ionic configurations were calculated up to an effective principal quantum number of 32. From Eq. (2), the index of refraction is obtained by multiplying the polarizability by the corresponding number density; that is

$$\mu - 1 = 2\pi \sum_i \sum_{j=1}^{ti} \frac{N_i}{Q_i} \alpha_j g_j e^{-Ej/kT}, \tag{7}$$

where i refers to the atoms and ions, j refers to the quantum level, N_i and Q_i are, respectively, the number density and internal partition function of the species, while g_j and E_j are, respectively, the degeneracy and energy level of the jth configuration, and k and T are the Boltzmann constant and plasma temperature, respectively. N_i and Q_i were found in Drellishak *et al*,[7] and the energy levels in Moore.[8] Individual terms of Eq. (7) are shown as a function of quantum level ($j \propto n$) in Fig. 1.

It is necessary to consider the termination of the sum in Eq. (7). An excited electron bound to an atom becomes free at the ionization limit of the atom. The energy associated with the ionization of argon is 127 110 cm^{-1} for an atom in an infinite volume. The electron-orbit radius at the ionization limit is infinite. For gas at moderate temperatures, the internuclear spacing is of the order of 10^{-6} cm. To estimate the lowering of the ionization potential the following approximations were used:

1. The influence of the nucleus is terminated at a radius r_H corresponding to one-half the internuclear spacing of the heavy particles[9]:

$$r_H = \tfrac{1}{2} N^{-1/3}, \tag{8}$$

where N is the number density of atoms and ions.

2. Debye-Hückel[10] described the termination radius r_D due to Coulomb interactions by

$$r_D = \left[\frac{kT\epsilon_0}{4\pi^2 e^2} 1/\sum N_i Q_i^2\right]^{1/2} = 6.88[T/\sum_i N_i Q_i^2]^{1/2} \text{ cm}, \tag{9}$$

where ϵ_0 is the free-space permittivity and i refers to the quantum level of the ith configuration.

At low temperatures the charge density is low, and the termination radius given by this relation will tend

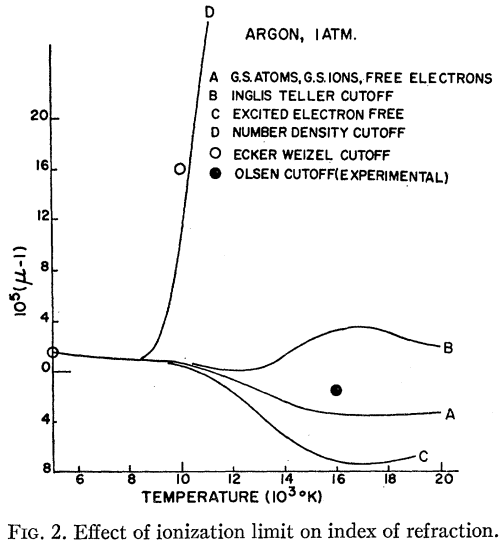

FIG. 2. Effect of ionization limit on index of refraction.

[4] A. C. Mitchell and M. W. Zemansky, *Resonance Radiation and Excited Atoms* (Cambridge University Press, Cambridge, England, 1961).
[5] R. S. Knox, Phys. Rev. **10**, 2 (1958).
[6] T. Gray, in *Smithsonian Physical Tables* (Smithsonian Institute Press, Washington, D. C., 1904).
[7] K. S. Drellishak, C. F. Knopp, and A. B. Cambel, Phys. Fluids **6**, 1280 (1963).
[8] C. E. Moore, Natl. Bur. Std. (U. S.) Circ. **467** (1949).
[9] H. N. Olsen, Phys. Rev. **124**, 1703 (1961).
[10] H. Margenau and M. Lewis, Rev. Mod. Phys. **31**, 569 (1959).

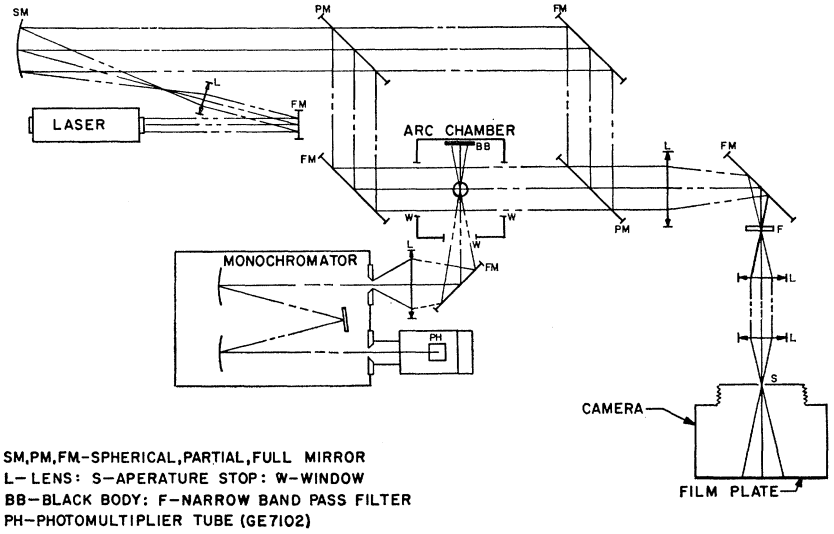

FIG. 3. Schema of apparatus.

toward infinity. Thus, at low temperatures, where Eq. (9) will give a termination radius that exceeds the internuclear spacing, the Deby-Hückel criterion will be invalid.

3. Inglis and Teller[11] described the termination principal quantum number due to broadening of the energy levels or merging of states. They give

$$\log_{10}N=23.3-7.5\log_{10}t. \tag{10}$$

4. Ecker and Weizel[12] describe the termination principal quantum number due to a "drowning of energy levels in the continuum." They give

$$t\simeq 3\times 10^{14}(N/T)^{-1/4}. \tag{11}$$

Unsöld's[13] theory describes a termination principal quantum number which is slightly smaller than that proposed by Inglis and Teller.

The effects of these various termination criteria on the calculated index of refraction are plotted in Fig. 2, where it is seen that the calculated index of refraction is strongly affected by the termination principal quantum number.

The Slater screening-constant method for calculating polarizabilities is expected to provide an upper value on the calculated index of refraction. The lower value is expected to be given when all of the bound electrons appear as free. However, it does not seem reasonable to include all bound electrons as free electrons at high temperatures. Curve C of Fig. 2 assumes that only the excited electron appears free to the illuminating wave, whereas the remaining more tightly bound electrons respond as they do in a cold gas. The assumption that the excited electron responds to the illuminating wave as if it were free is, in essence, terminating the influence of the nucleus on an excited electron at the ground state.

III. EXPERIMENT

Two devices were used in these experiments to produce a plasma: a modified commercial plasma jet which discharged into the atmosphere, and a free-burning arc. The free-burning arc has the advantage that a hotter, more stable plasma sample is produced. The modifications to the plasma jet used here were previously described.[14] The free-burning arc is com-

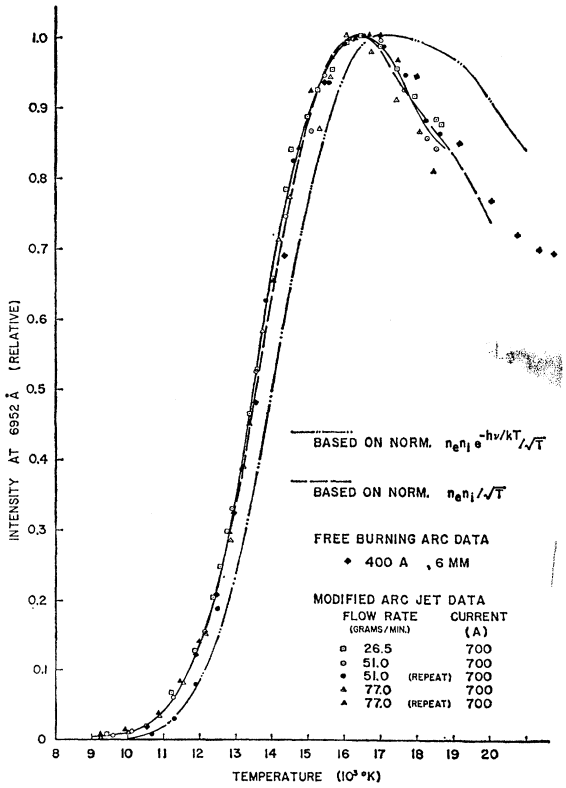

FIG. 4. Continuum radiation versus temperature.

[11] D. R. Inglis and E. Teller, Astrophys. J. **90**, 439 (1939).
[12] G. Ecker and W. Weizel, Ann. Physik **17**, 126 (1956).
[13] A. Unsöld. Ann. Phvsik **33**. 607 (1938).
[14] W. F. Hug, D. L. Evans, R. S. Tankin, and A. B. Cambel, Office of Aerospace Research, U. S. Air Force, Report No. ARL66-0140 (1966) (unpublished).

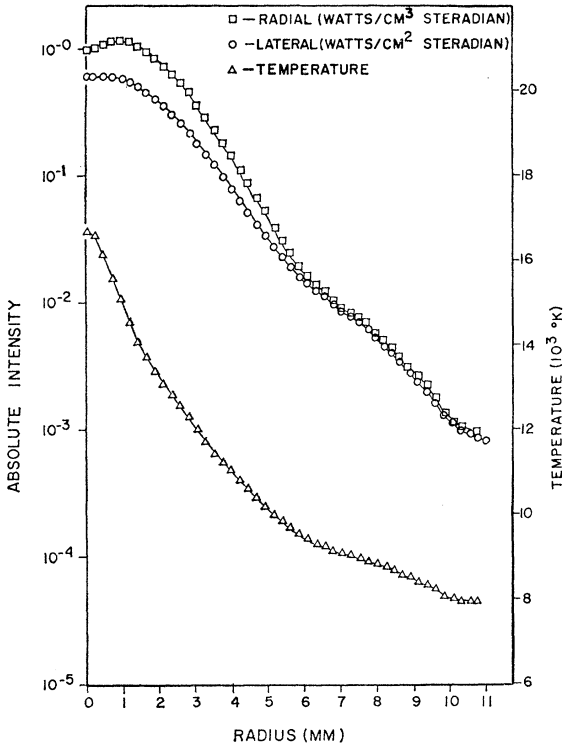

FIG. 5. Radial intensity and temperature profiles.

posed of a pointed 3.18-mm-diam water-cooled 1% thoriated tungsten cathode and a flat 19-mm-diam water-cooled copper anode. Anode and cathode are coaxially spaced at 6 mm. The arc current was maintained at 250 A in high-purity dry argon gas at 1.10 atm.

Spectroscopic measurements to find temperature and verify local thermal equilibrium (LTE) in the arc and jet were made with a ¾ meter Czerny-Turner–type monochromator. Horizontal and vertical entrance slits provided an object resolution size of 0.02 mm by 0.025 mm. A cooled GE 7102 photomultiplier tube is used to measure light output from the exit slit. Interferometric measurements were made with a Mach-Zehnder–type interferometer with ¼ wave (sodium D) optics with a field size of 20 cm by 13 cm. A helium-neon laser with beam expanded to about 10 cm was used to illuminate the plasma through the interferometer. Figure 3 illustrates the arrangement of the apparatus.

Radial distributions of temperature and index of refraction at different levels between anode and cathode are found from lateral distributions of spectral line intensity and phase shift using Abel integral inversion. In order for the Abel inversion to be used, axial symmetry is assumed. The amount of asymmetry was determined by folding the lateral distributions about the centerline of the plasma source. The maximum difference between the two half-distributions at any lateral position was less than 2% of the value at the centerline.

Throughout the calculations it is assumed that in the plasma there exists an equilibrium distribution of energy between species, atomic and ionic state populations, and species densities. Since the electric fields maintaining the arc are small, the species are expected to be at the same temperature.[15]

Equilibrium species densities and state populations are validated by comparing experimental relative continuum intensities as a function of temperature with the Kramer-Unsöld theory. This was done by cross plotting the radial continuum-intensity distribution at 6920Å with the radial temperature distribution found by the Fowler-Milne[15] technique from the 6965Å argon atom line. The low-level excited states are generally more difficult to equilibrate than high-level excited states. Since the 6965AI line is due to a low-level excited state, its equilibrium is expected to indicate

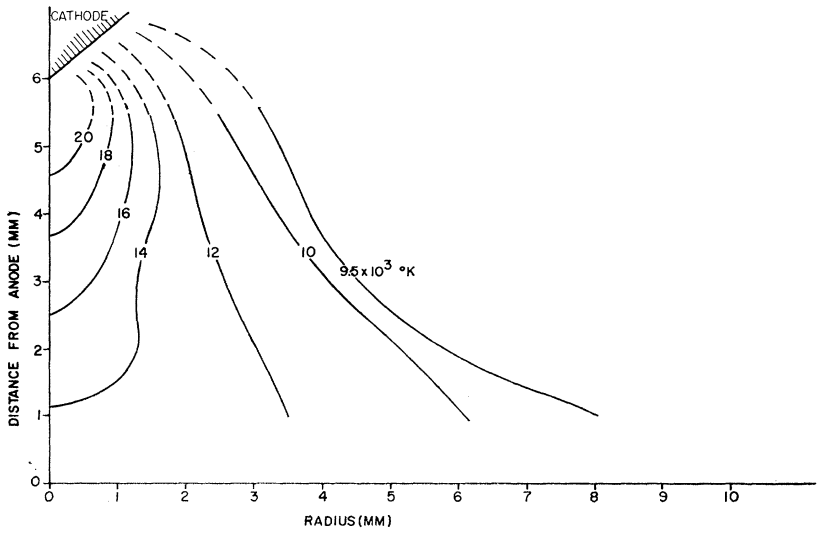

FIG. 6. Free-burning arc isotherms.

[15] C. F. Knopp, C. Gottschlich, and A. B. Cambel, J. Quant. Spectr. Radiative Transfer 2, 297 (1962).

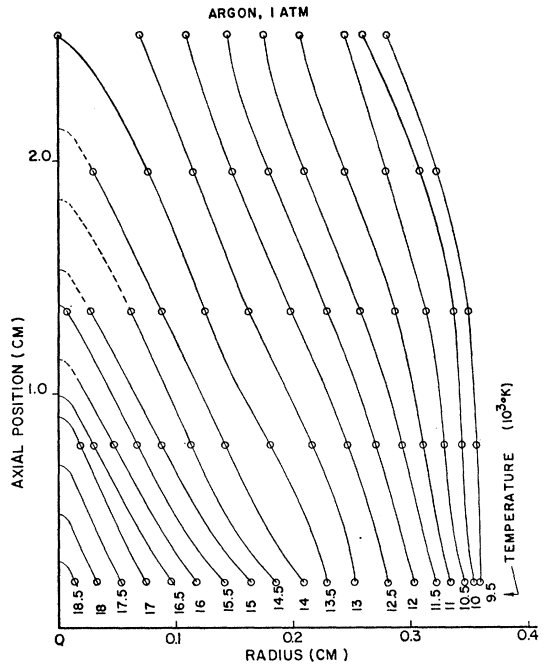

FIG. 7. Arc-jet isotherms.

equilibrium for all higher-state population.[16] Figure 4 shows that the continuum intensity (proportional to $N_e N_i/\sqrt{T}$) calculated assuming LTE is in excellent agreement with measured values. In Fig. 4, N_e, N_i, and T refer to electron and first-ion number densities and temperature, respectively. Hence, LTE appears justified.

The 6965.43 AI line was chosen for temperature measurements because of its isolation from neighboring lines. The vertical entrance slit was set at 0.01 mm and the exit slit to 1.75 mm, giving a spectral bandpass of 18.4 Å, so that any broadening or shifting of the line in the plasma will remain within the band pass viewed. Lateral-intensity distributions were taken at wavelengths centered at 6920, 6965, and 7010 Å. The average of the continuum measurements (6920 and 7010 Å) was assumed to be the continuum distribution under the line plus continuum measured at 6965 Å. The average continuum was subtracted at each lateral position from the distribution at 6965 Å, yielding the line-intensity distribution.

The radial line-intensity distributions were obtained using the Nestor-Olsen[17]-Abel inversion technique.

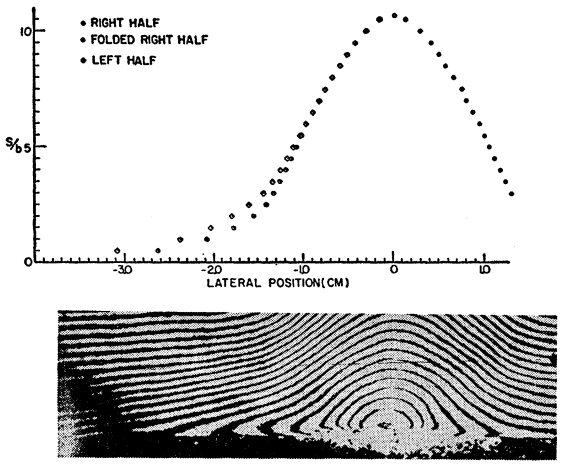

FIG. 8. Arc-jet interferogram.

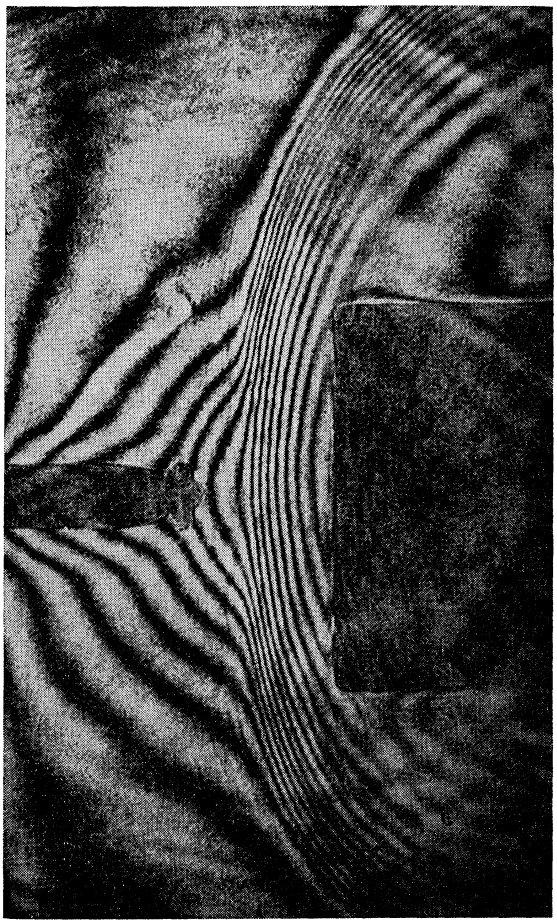

FIG. 9. Free-burning arc interferogram.

Temperatures were then obtained using the Fowler-Milne technique.[15] A typical distribution is shown in Fig. 5.

It has been shown[18] that temperatures obtained by this technique are nearly independent of self-absorption in the plasma. The maximum statistical error in the measurement of temperature was determined to be 3%. This corresponds to about a 20% error in electron

[16] R. Wilson, J. Quant. Spectr. Radiative Transfer **2**, 477 (1962).

[17] O. H. Nestor and H. N. Olsen, Soc. Ind. Appl. Math. Rev. **2**, 300 (1960).

[18] D. Evans and R. S. Tankin, Phys. Fluids **10**, 1137 (1967).

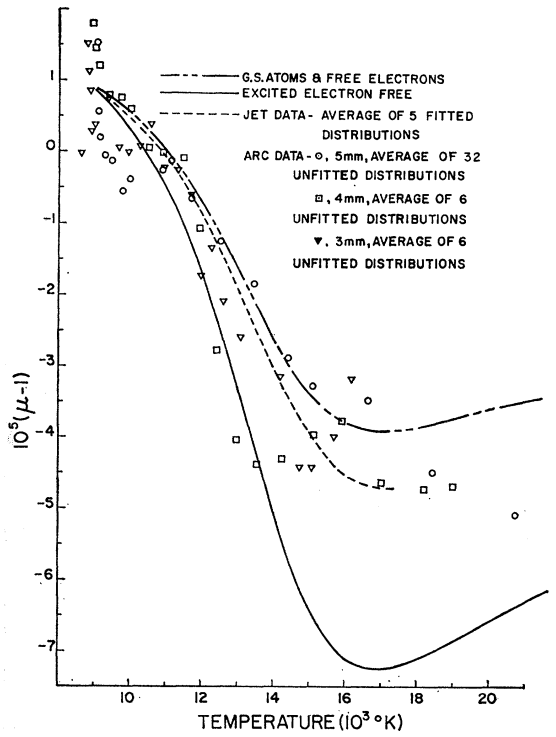

FIG. 10. Experimental index of refraction.

density at 10 000°K and 2% at 16 000°K. Isotherms in the arc and jet are shown in Figs. 6 and 7, respectively.

The radial index-of-refraction distribution in the plasma was determined from the lateral distribution of phase shift of the light illuminating the plasma through the interferometer. The phase shift of a ray passing through the plasma is

$$\int_0^L (\mu-\mu_0)dl=\lambda S, \qquad (12)$$

where L is the chord length through the plasma, dl is an increment of this length, μ is the index of refraction in the plasma, μ_0 is some reference index of refraction, λ is the illumination wavelength, and S is the phase shift of the ray traversing the plasma.

Numerous interference-fringe orientations are available for describing the phase-shift distribution through the plasma. In each of these the comparison is made between the lateral-fringe distribution with the plasma source on and off. The interference fringe intensity pattern is not sinusoidal because of additional modulation of the intensity due to nonuniformities in the illumination laser beam as well as the optics. The most serious modulation of the pattern is produced by the narrow bandpass filter. The filter is necessary in order to reduce the intense radiation from the plasma to a level where the exposure of the film from the laser radiation predominates over the exposure from the plasma radiation. In the case of the jet interferograms, the plasma radiation was reduced to a tolerable level with a filter having a bandpass of 150 Å. This filter did not produce serious modulation and offered sufficient resolving power on phase shift through the plasma. An example is shown in Fig. 8. In the case of the arc interferograms it was necessary to use a filter with a bandpass of 16 Å. The amount of modulation produced by this filter allowed the accurate location of only the maximum and minimum intensity points on the fringe. Figure 9 illustrates an infinite fringe interferogram showing the arc symmetry and isophase shift contours.

The maximum resolution on the spacial distribution of phase shift is achieved by making the fringe as narrow as is conveniently recordable on film. For the data recorded here this resolution was approximately 0.2 mm per fringe in the arc. The lateral fringe positions were measured with a constant-scanning speed densitometer whose output was recorded on a strip-chart recorder. Positions of maximum and minimum intensity of the fringe (density on the film) were measured while scanning the interferogram normal to the plasma source axis. To eliminate any phase distortion due to the optics, the fringe distribution at a given level between anode and cathode was measured with the plasma source off. This distribution for the jet data was curve-fitted and subtracted at each lateral position from the curve-fitted fringe distribution with the jet turned on. In the case of the arc data, the fringe distributions for arc on and arc off were not curve fitted. This difference yields the lateral phase-shift distribution with a high-degree resolution. The distributions are folded about the source centerline to check symmetry and inverted using the Abel integral inversion. To obtain the absolute index-of-refraction distribution it was assumed that the index of refraction at 11 000°K was equal to the value calculated using only ground-state atoms and free electrons. The result of cross plotting the radial distributions of index of refraction and temperature are shown in Fig. 10.

IV. CONCLUSIONS

From the experimental data it is seen that the index of refraction is lower than that predicted by considering only ground-state atoms and free electrons as contributors. Since excited electrons are present in sufficient quantities to be measurable, the method of their inclusion into the theory requires a balance between the free-electron negative-contributors and the excited-electron positive-contributors. The lower theoretical curve in Fig. 10 is a result of essentially lowering the ionization limit to the ground state. It appears that the excited electrons provide the difference between this curve and the experimental data.

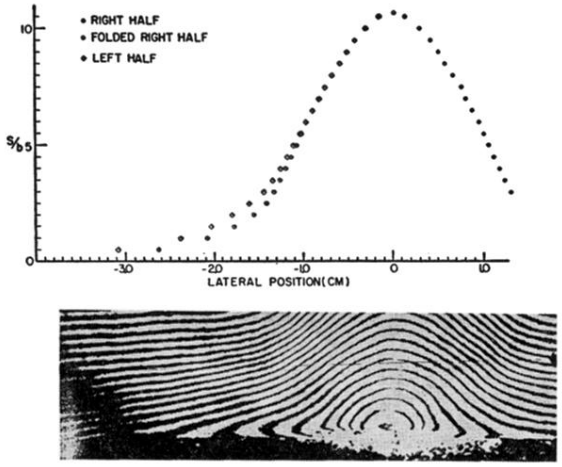

FIG. 8. Arc-jet interferogram.

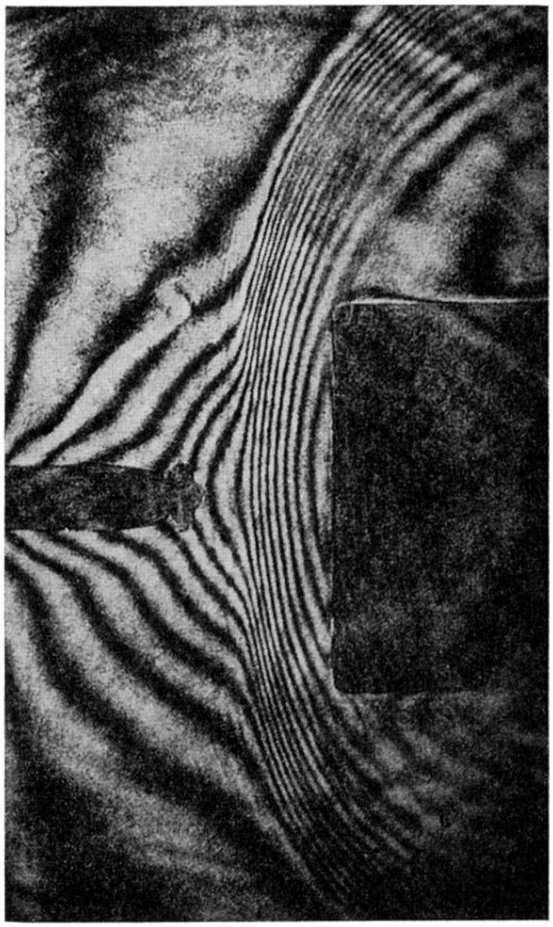

FIG. 9. Free-burning arc interferogram.